PHYSICAL REVIEW B **87**, 020506(R) (2013)

Ferroelectric soft phonons, charge density wave instability, and strong electron-phonon coupling in BiS_2 layered superconductors: A first-principles study

T. Yildirim*

NIST Center for Neutron Research, National Institute of Standards and Technology, Gaithersburg, Maryland 20899, USA and Department of Materials Science and Engineering, University of Pennsylvania, Philadelphia, Pennsylvania 19104, USA

(Received 25 October 2012; published 17 January 2013)

Very recently a new family of layered materials, containing BiS_2 planes, was discovered to be superconducting at temperatures up to $T_c = 10$ K, raising questions about the mechanism of superconductivity in these systems. Here, we present state-of-the-art first-principles calculations that directly address this question and reveal several surprising findings. The parent compound $LaOBiS_2$ possesses anharmonic ferroelectric soft phonons at the zone center with a rather large polarization of $\approx 10\ \mu C/cm^2$. Upon electron doping, new unstable phonon branches appear along $Q = (q,q,0)$, causing Bi/S atoms to order in a one-dimensional charge density wave (CDW). We find that BiS_2 is a strong electron-phonon coupled superconductor in the vicinity of competing ferroelectric and CDW phases. Our results suggest directions to increase T_c in this new class of materials.

DOI: 10.1103/PhysRevB.87.020506 PACS number(s): 74.25.Jb, 63.20.kd, 74.20.Pq, 77.80.B−

Superconductivity, a phenomenon first documented in 1911, remains one of the most challenging subjects of condensed matter physics. Examples of layered superconductors include cuprates,[1] MgB_2,[2] CaC_6,[3] and recent iron pnictides.[4] Very recently a new family of layered materials, $Bi_4O_4S_3$[5] and $RO_xF_{1-x}BiS_2$ (R = La, Nd, Pr, and Ce),[6–9] containing BiS_2 planes, was discovered to be superconducting at temperatures up to 10 K. These new systems are structurally similar to the layered, iron-based superconductors $LaO_xF_{1-x}FeAs$,[4] and in both cases the superconductivity is achieved by F doping. In addition, band structure calculations[10,11] indicate the presence of strong Fermi surface nesting at the wave vector (π,π), which is the hallmark property of the Fe pnictides.[12,13] These similarities have raised the exciting question of whether or not the superconducting mechanism in the BiS_2 system is related to that in the iron pnictides, and this has therefore generated enormous interest.[5–11,14–20]

The fundamental question is whether or not the observed T_c in this new system can be understood within a conventional electron-phonon coupling framework, or is a more exotic mechanism responsible for the superconducting pairing? In this Rapid Communication, we present state-of-the-art first-principles calculations that directly address this question and reveal several surprising findings, such as anharmonic ferroelectric soft phonons and one-dimensional charge density wave (CDW) instability. The technical details of the calculations[21–23] are given in the Supplemental Material (SM).[24]

Figure 1 shows the $P4/nmm$ tetragonal cell of the $LaO_xF_{1-x}BiS_2$, which consists of two types of atomic layers, namely, the LaO spacer and electronically active BiS_2 bilayer. Upon F doping in the LaO layer, one can control the charge transfer to the BiS_2 bilayer and thus tune the electronic properties. In order to simulate such doping in our calculations, we generated a $2 \times 2 \times 1$ supercell of $LaOBiS_2$ and replaced some of the oxygen atoms with F atoms in an ordered fashion with doping levels of $x = 0$, 0.125, 0.25, 0.375, and 0.5. The results are summarized in Fig. 2.

The undoped parent compound is a band insulator with a gap of $\approx$0.8 eV. Upon electron doping, we start to fill the empty states in a rigid-band fashion, turning the insulating parent compound into a metallic system. From the projected density of states (DOS), we determine that the states near the Fermi level are mainly of Bi $6p$ and S $3p$ character. The density of states at the Fermi level $N(E_F)$ increases with increasing electron doping and becomes maximal at the half filing $x = 0.5$. In agreement with experiments, the c-axis length decreases while the a- and b-axis lengths increase with F doping. Interestingly, the z values of the in-plane S (i.e., S_{in}) and Bi atoms get closer to each other with doping, yielding a nearly perfect planar structure at $x = 0.5$. On the other hand, zigzag buckled planes are formed at $x = 0$, as shown in Fig. 1. This rearrangement of Bi and S atoms into a perfect planar structure should have important consequences for the

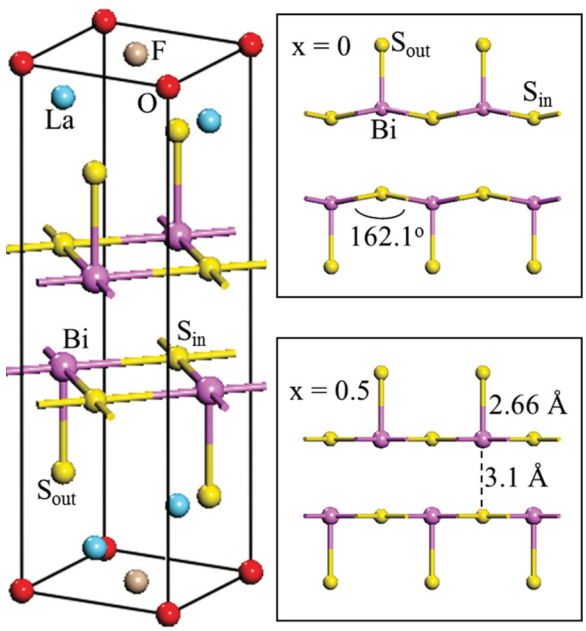

FIG. 1. (Color online) Crystal structure of $LaO_xF_{1-x}BiS_2$ ($x = 0.5$). The side views of the BiS_2 bilayer for $x = 0$ (top) and $x = 0.5$ (bottom) are also shown. Note the zigzag pattern of the BiS_2 plane for $x = 0$.

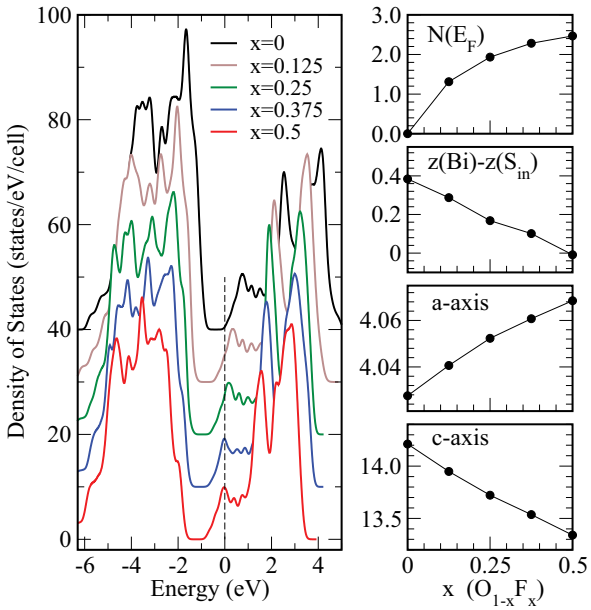

FIG. 2. (Color online) Electronic DOS of $LaO_xF_{1-x}BiS_2$ as a function of F doping x. For clarity the curves are shifted vertically except $x = 0.5$. On the right, $N(E_F)$ (scaled per 10-atom unit cell), lattice parameters, and the difference of the z values (all in Å) of in-plane S (S_{in}) and Bi atoms are also given.

electronic band structure and the nature of the Fermi surface. Hence it is important to keep an eye on the degree of buckling of the BiS_2 plane and its relation to T_c as new isostructural materials are being discovered. We note that similar buckling of the CuO_2 plane in cuprates with doping was found to be closely correlated with the superconducting temperature.[25]

One of the most interesting results shown in Fig. 2 is that $N(E_F)$ is quite high at half filling ($x = 0.5$) and E_F coincides with a peak in the density of states. This usually suggests some sort of instability due to a Van Hove singularity. In order to check this, we calculated phonon dispersion curves of the parent ($x = 0$) and half-doped ($x = 0.5$) systems using a $4 \times 4 \times 1$ supercell, and the results are shown in Fig. 3. To our surprise, we find that the undoped system shows instability near Γ while the doped system has instabilities along the entire line of $Q = (q,q,0)$ [see also Fig. S2 in the SM (Ref. 24)]. We repeated the phonon dispersion calculations for $x = 0.5$ using a charged system without F doping and obtained the same instabilities [see Fig. S1 in the SM (Ref. 24)], indicating that the soft phonons found here are an intrinsic property of the BiS_2 plane.

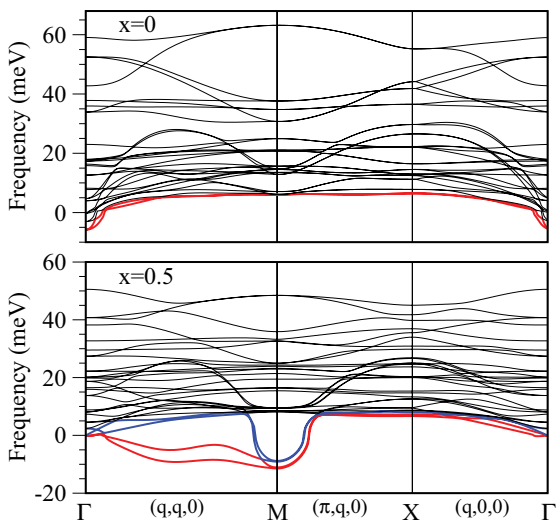

FIG. 3. (Color online) Phonon dispersion curves of $LaOBiS_2$ (top) and $LaO_{0.5}F_{0.5}BiS_2$ (bottom), indicating the instabilities at Γ for $x = 0$ and along the entire line $(q,q,0)$ with the most unstable phonons at M and $(\pi/2,\pi/2)$ for $x = 0.5$.

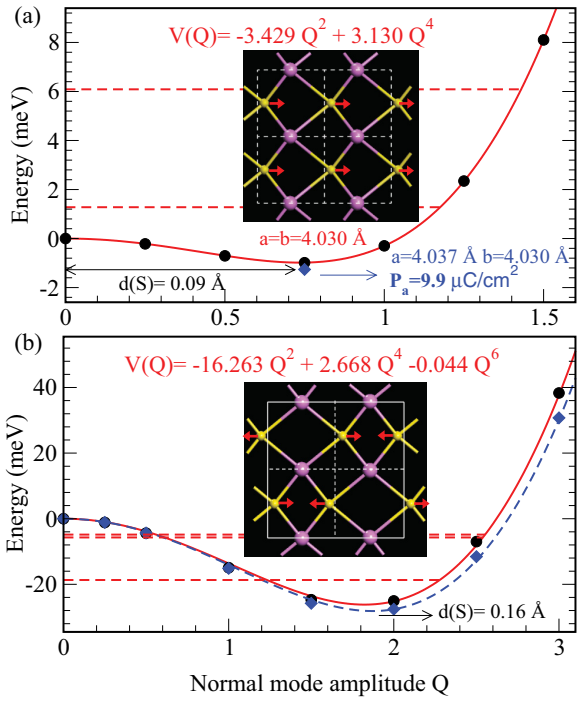

FIG. 4. (Color online) Total energy as the system is distorted by the most negative energy phonons in the tetragonal cell of $LaOBiS_2$ at Γ (a) and in the $\sqrt{2} \times \sqrt{2}$ cell of $LaO_{0.5}F_{0.5}BiS_2$ at $M(\pi,\pi)$ (b). The insets show the sketch of the unstable phonons. The horizontal dashed red lines show the energy levels of the frozen-phonon potential (red curve).

In order to have a better insight into the nature of these unstable phonons, we carried out total energy calculations as the system was distorted by the modes having the most negative energy. Figure 4(a) shows the most unstable soft phonon E_u at Γ for $x = 0$, which lowers the symmetry from $P4/nmm$ to $P21mn$. The S atoms move towards Bi atoms along the a axis (or b axis) and slightly lower the energy of the system by ≈1 meV. When the lattice parameters are relaxed, the tetragonal cell becomes orthorhombic and the system energy is further lowered by 0.3 meV. The final structure is shown in Fig. S3.[24] It is remarkable that in the distorted phase, the inversion symmetry is broken and a large spontaneous polarization of $P = 9.9\ \mu C/cm^2$ is induced despite the rather small displacements. The calculated polarization is comparable to that of the well-known room temperature ferroelectric $BiFeO_3$ system.[26] However, we note that the potential curve for this unstable ferroelectric phonon mode is quite shallow, as shown in Fig. 4, and quantum zero-point motions may not allow such structural distortion. In fact, solving the Schrödinger equation for this potential, we obtained energy levels which

are above the potential minimum. Hence, the system should be dynamically disordered due to zero-point motions and should appear as tetragonal. These findings seem to be consistent with the room temperature x-ray data reported so far. Finally, we suggest that the origin of the anharmonic ferroelectric mode could be due to a mismatch between the optimum lattice parameters of the LaO and the BiS_2 layers. If the Bi-S bond is forced to elongate due to an interaction between the LaO and BiS_2 planes, then it is natural for the S atom to break the symmetry and move towards the Bi atom to optimize the Bi-S interaction. In fact, repeating the phonon calculations for smaller lattice parameters (i.e., $a = b = 3.8$ Å, corresponding to 100 kbar pressure), we no longer get negative phonon energies at the zone center. Hence, it seems that by changing the spacer oxide, one may tune the nature of the soft phonons and the ground state structure.

Figure 4(b) shows the total energy in the $\sqrt{2} \times \sqrt{2}$ cell of the tetragonal structure for $x = 0.5$ as it is distorted by the most negative energy phonon mode at (π,π). Unlike the parent compound, the distortion lowers the system energy significantly, causing S atoms to move away by 0.16 Å from the high symmetry site. Solving numerically the Schrödinger equation for the resulting potential curve, we obtained the energy levels which are bound to the local minimum of the distortion. The dashed line in Fig. 4(b) shows that the same distortion also occurs for the charged system without F doping. Hence, the observed soft mode is an intrinsic property of the BiS_2 plane. We next checked whether the (π,π) phonon optimized $\sqrt{2} \times \sqrt{2}$ structure is stable at other q vectors by repeating the phonon calculations using a $2\sqrt{2} \times 2\sqrt{2}$ supercell. We obtained more negative energy modes that correspond to the original instability at the $(\pi/2,\pi/2)$ of the $4 \times 4 \times 1$ tetragonal supercell calculations. Hence, we further distorted the $2\sqrt{2} \times 2\sqrt{2}$ structure by the $(\pi/2,\pi/2)$ negative energy phonon and let the system relax. We determined that the optimized structure has a $\sqrt{2} \times 2\sqrt{2}$ unit cell with a rather interesting rearrangement of Bi and S atoms in the BiS_2 plane, as shown in Figs. 5 and S4 (see Ref. 24). We call this distorted structure the CDW phase, due to the sinusoidal distortion of the Bi and S atoms, as shown by the red dashed lines in Fig. 5. Unlike the $x = 0$ case, applying pressure or using smaller lattice constants in the phonon calculations does not stabilize the negative energy phonons. Hence, it is tempting to conclude that the origin of this distortion is due to strong Fermi surface nesting at M.[10,11] However, we note that the soft phonon branch occurs along the entire line $Q = (q,q,0)$ and not just at the M point. Hence, in addition to Fermi surface nesting, there should be an important structural reason as well for the observed soft modes. Finally, by looking at the bond distances between Bi-S, we notice that there are one-dimensional channels of Bi-S bonding, as shown in Fig. 5. Interestingly, from Hall effect measurements[16] it was concluded that superconducting pairing occurs in one-dimensional chains in these systems, which could be related to the CDW phase predicted here. Similarly, high pressure measurements reveal a nonmonotonic dependence of T_c on pressure and suggest that the Fermi surface of $LaO_xF_{1-x}BiS_2$ could be in the vicinity of instabilities.[14] Finally, the x-ray powder diffraction[6] for $LaO_{0.5}F_{0.5}BiS_2$ shows rather unusual broad peaks, which could be again related to the CDW phase.

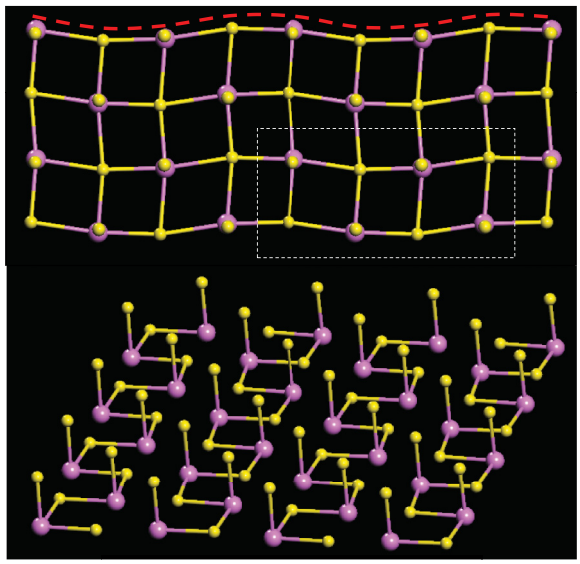

FIG. 5. (Color online) The BiS_2 plane in a fully optimized CDW phase of $LaO_{0.5}F_{0.5}BiS_2$. Large (pink) and small (yellow) spheres are Bi and S, respectively. The dashed (red) line is to guide the eye, indicating the sinusoidal distortion of the atoms. The white square indicates the $2\sqrt{2} \times \sqrt{2}$ unit cell of the CDW phase. The bottom panel shows the same structure with a Bi-S bond cutoff distance of 2.8 Å. The one-dimensional nature of the chains becomes apparent. The intrachain Bi-S bond is about 2.75 Å while the interchain Bi-S bond is around 3 Å [see Fig. S3 (Ref. 24)].

We next address the nature of superconductivity found in these BiS_2 layered systems. We carried out electron-phonon (el-ph) coupling calculations using both (π,π)-phonon optimized $\sqrt{2} \times \sqrt{2}$ and CDW structures. We consider $2\sqrt{2} \times 2\sqrt{2}$ supercells, containing 80 atoms, and obtain the el-ph coupling by the frozen-phonon method. Two negative energy modes of the (π,π)-phonon optimized structure were not included in the el-ph coupling calculations. The results are summarized in Fig. 6. In both (π,π)-optimized or fully distorted CDW structures, the Eliashberg functions are quite similar, indicating that the main physics of the electron-phonon coupling mechanism does not depend on the details of the structure. In the (π,π)-phonon optimized structure, $N(E_F)$ is higher than in the CDW phase [see Fig. S5 (Ref. 24)], and therefore leads to higher el-ph coupling. The total electron-phonon coupling is $\lambda = 0.83$ with a logarithmic frequency average $\omega_{\log} = 101$ K. These values give a maximum superconducting temperature of $T_c = 8.5$ K. Even in the fully distorted CDW phase, we get quite large electron-phonon coupling $\lambda = 0.6$ and a logarithmic frequency average $\omega_{\log} = 122$ K, which gives a T_c of 6 K. The other values of T_c-μ^* are plotted in Fig. S6.[24] These values are in good agreement with the reported experimental values of T_c which vary from 3 to 10 K, depending on the level of doping and sample quality. Inspecting the modes which give the highest el-ph coupling, we estimate that about 90% of λ comes from in-plane Bi and S phonons while the remaining 10% is due to phonons along the c axis. There are two bands of phonons near 5–10 and 15–25 meV. The phonons in the lower energy band are due to coupled Bi and S motion while the phonons in the high energy

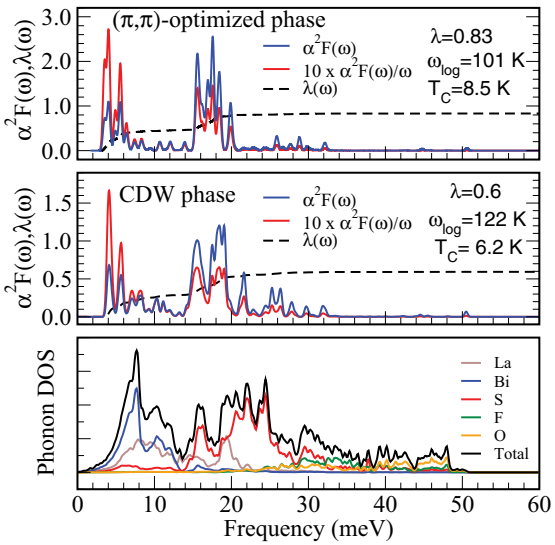

FIG. 6. (Color online) Eliashberg functions in a partially optimized (top) and fully optimized CDW structure (middle). el-ph coupling constants $\lambda, T_c, \omega_{\log}$ are also given. The total and atomic-projected phonon DOS in the CDW phase are shown in the bottom panel.

bands are due to almost pure S oscillations. An animation of these modes can be found in Ref. 27. In Fig. 6, we also show the total phonon density of states along with the atomic projections of the DOS. As expected, based on the masses of atoms, O- and F-based phonons are above 30 meV and do not produce much el-ph coupling. The La phonons are near 10 meV but, as expected, do not produce any significant el-ph coupling.

In conclusion, we have discovered rather unusual structural and dynamical properties of $LaOBiS_2$ with electron doping. The large-amplitude in-plane S-atom displacement controls the structural properties and gives rise to large el-ph coupling. It would be interesting to measure the isotope effect for the S atom, which may be unconventional. Our results also suggest that thin films of BiS_2 on various substrates may exhibit unusual properties due to epitaxial strain at the interface. New materials with similar structures but with a BiO_2 plane could be quite interesting due to the smaller mass of the oxygen atom, which gives higher phonon energies, and in turn higher T_c. In fact, the results reported here remind us of another interesting system, namely, $Ba_{1-x}K_xBiO_3$,[28,29] which exhibits several complicated structural phases[29] and superconductivity at 31 K.[28] Our results clearly indicate that the BiS_2-based layered systems are very rich in physics, involving nearly ferroelectric soft phonons and CDW ordering along with strongly coupled electron-phonon superconductivity.

We acknowledge many fruitful discussions with A. B. Harris and P. M. Gehring.

*taner@seas.upenn.edu

[1] J. Orenstein and A. J. Millis, Science **288**, 468 (2000).
[2] J. Nagamatsu, N. Nakagawa, T. Muranaka, Y. Zenitani, and J. Akimitsu, Nature (London) **410**, 63 (2001).
[3] T. E. Weller, M. Ellerby, S. S. Saxena, R. P. Smith, and N. T. Skipper, Nat. Phys. **1**, 39 (2005).
[4] H. Takahashi, K. Igawa, K. Arii, Y. Kamihara, M. Hirano, and H. Hosono, Nature (London) **453**, 376 (2008).
[5] Y. Mizuguchi, H. Fujihisa, Y. Gotoh, K. Suzuki, H. Usui, K. Kuroki, S. Demura, Y. Takano, and H. Izawa, and O. Miura, Phys. Rev. B **86**, 220510(R) (2012).
[6] Y. Mizuguchi, S. Demura, K. Deguchi, Y. Takano, H. Fujihisa, Y. Gotoh, H. Izawa, and O. Miura, J. Phys. Soc. Jpn. **81**, 114725 (2012).
[7] S. Demura, Y. Mizuguchi, K. Deguchi, H. Okazaki, H. Hara, T. Watanabe, S. J. Denholme, M. Fujioka, T. Ozaki, H. Fujihisa, Y. Gotoh, O. Miura, T. Yamaguchi, H. Takeya, and Y. Takano, arXiv:1207.5248.
[8] R. Jha, A. Kumar, S. K. Singh, and V. P. S. Awana, arXiv:1208.5873.
[9] J. Xing, S. Li, X. Ding, H. Yang, and H. H. Wen, Phys. Rev. B **86**, 214518 (2012).
[10] H. Usui, K. Suzuki, and K. Kuroki, arXiv:1207.3888.
[11] X. Wan, H. Ding, S. Y. Savrasov, and C. Duan, arXiv:1208.1807.
[12] J. Dong, H. J. Zhang, G. Xu, Z. Li, G. Li, W. Z. Hu, D. Wu, G. F. Chen, X. Dai, J. L. Luo, Z. Fang, and N. L. Wang, Europhys. Lett. **83**, 27006 (2008).
[13] I. I. Mazin, D. J. Singh, M. D. Johannes, and M. H. Du, Phys. Rev. Lett. **101**, 057003 (2008).
[14] H. Kotegawa, Y. Tomita, H. Tou, H. Izawa, Y. Mizuguchi, O. Miura, S. Demura, K. Deguchi, and Y. Takano, J. Phys. Soc. Jpn. **81**, 103702 (2012).
[15] T. Zhou and W. Z. Wang, J. Supercond. Novel Magn. (2012), doi: 10.1007/s10948-012-2073-4.
[16] S. Li, H. Yang, J. Tao, X. Ding, and H. Wen, arXiv:1207.4955.
[17] V. P. S. Awana, A. Kumar, R. Jha, S. Kumar, A. Pal Shruti, J. Saha, and S. Patnaik, arXiv:1207.6845.
[18] H. Takatsu, Y. Mizuguchi, H. Izawa, O. Miura, and H. Kadowaki, J. Phys. Soc. Jpn. **81**, 125002 (2012).
[19] C. I. Sathish and K. Yamaura, arXiv:1208.2818.
[20] H. Lei, K. Wang, M. Abeykoon, E. S. Bozin, and C. Petrovic, arXiv:1208.3189.
[21] P. Giannozzi *et al.*, J. Phys.: Condens. Matter **21**, 395502 (2007).
[22] P. E. Blochl, Phys. Rev. B **50**, 17953 9 (1994).
[23] P. K. Lam, M. M. Dacorogna, and M. L. Cohen, Phys. Rev. B **34**, 5065 (1986).
[24] See Supplemental Material at http://link.aps.org/supplemental/10.1103/PhysRevB.87.020506 for the details of methods and additional plots of the phonon dispersion curves, picture of optimized structures, and atomic positions and lattice parameters.
[25] O. Chmaissem, J. D. Jorgensen, S. Short, A. Knizhnik, Y. Eckstein, and H. Shaked, Nature (London) **397**, 45 (1999).
[26] C. Ederer and N. A. Spaldin, Phys. Rev. Lett. **95**, 257601 (2005).
[27] Animations of the phonons that give the largest el-ph coupling in $LaO_xF_{1-x}BiS_2$ can be found at http://www.ncnr.nist.gov/staff/taner/LaOBiS2.
[28] R. J. Cava, B. Batlogg, J. J. Krajewski, R. Farrow, L. W. Rupp, Jr., A. E. White, K. Short, W. F. Peck, and T. Kometani, Nature (London) **332**, 814 (1988).
[29] M. Braden, W. Reichardt, E. Elkaim, J. P. Lauriat, S. Shiryaev, and S. N. Barilo, Phys. Rev. B **62**, 6708 (2000).